# LETTERS

# Control of chromosome stability by the β-TrCP–REST–Mad2 axis

Daniele Guardavaccaro[1], David Frescas[1], N. Valerio Dorrello[1], Angelo Peschiaroli[1], Asha S. Multani[3], Timothy Cardozo[2], Anna Lasorella[4], Antonio Iavarone[4], Sandy Chang[3], Eva Hernando[1] & Michele Pagano[1]

REST/NRSF (repressor-element-1-silencing transcription factor/neuron-restrictive silencing factor) negatively regulates the transcription of genes containing RE1 sites[1,2]. REST is expressed in non-neuronal cells and stem/progenitor neuronal cells, in which it inhibits the expression of neuron-specific genes. Overexpression of REST is frequently found in human medulloblastomas and neuroblastomas[3–7], in which it is thought to maintain the stem character of tumour cells. Neural stem cells forced to express REST and c-Myc fail to differentiate and give rise to tumours in the mouse cerebellum[3]. Expression of a splice variant of REST that lacks the carboxy terminus has been associated with neuronal tumours and small-cell lung carcinomas[8–10], and a frameshift mutant (REST-FS), which is also truncated at the C terminus, has oncogenic properties[11]. Here we show, by using an unbiased screen, that REST is an interactor of the F-box protein β-TrCP. REST is degraded by means of the ubiquitin ligase SCF$^{β-TrCP}$ during the G2 phase of the cell cycle to allow transcriptional derepression of *Mad2*, an essential component of the spindle assembly checkpoint. The expression in cultured cells of a stable REST mutant, which is unable to bind β-TrCP, inhibited *Mad2* expression and resulted in a phenotype analogous to that observed in *Mad2$^{+/−}$* cells. In particular, we observed defects that were consistent with faulty activation of the spindle checkpoint, such as shortened mitosis, premature sister-chromatid separation, chromosome bridges and mis-segregation in anaphase, tetraploidy, and faster mitotic slippage in the presence of a spindle inhibitor. An indistinguishable phenotype was observed by expressing the oncogenic REST-FS mutant[11], which does not bind β-TrCP. Thus, SCF$^{β-TrCP}$-dependent degradation of REST during G2 permits the optimal activation of the spindle checkpoint, and consequently it is required for the fidelity of mitosis. The high levels of REST or its truncated variants found in certain human tumours may contribute to cellular transformation by promoting genomic instability.

F-box proteins are the substrate-recognition subunits of SCF (SKP1–CUL1–F-box protein) ubiquitin ligases, providing specificity to ubiquitin conjugation reactions[12,13]. Mammals express two paralogues of the F-box protein β-TrCP (β-TrCP1 and β-TrCP2) that are biochemically indistinguishable; we shall therefore use β-TrCP to refer to both, unless otherwise specified.

To identify substrates of the SCF$^{β-TrCP}$ ubiquitin ligase, we used an immunoaffinity/enzymatic assay followed by mass spectrometry analysis[14,15]. In two independent purifications, peptides corresponding to REST were identified. The interaction between REST and β-TrCP suggested that SCF$^{β-TrCP}$ is the ubiquitin ligase targeting REST for degradation. To investigate the specificity of this binding, we screened 16 F-box proteins as well as two related proteins, CDH1

and CDC20. β-TrCP1 and β-TrCP2 were the only proteins that immunoprecipitated together with endogenous REST (Fig. 1a and data not shown). Interaction between endogenous β-TrCP1 and REST was also observed (Supplementary Fig. 1a).

Most proteins recognized by β-TrCP contain a DSGXXS degron in which the serine residues are phosphorylated, allowing binding to β-TrCP[16]. REST has a similar motif at the C terminus in which the first serine residue is replaced by glutamic acid, in an analogous manner to other known β-TrCP substrates (Supplementary Fig. 2a). Supplementary Fig. 3 shows that this sequence fits with low energy into the three-dimensional structural space of the β-TrCP substrate-binding surface, similarly to a phospho-peptide corresponding to the degron of β-catenin, a well-characterized substrate of β-TrCP[17].

We generated a number of human REST mutants (all with haemagglutinin epitope (HA) tags), in which Glu 1009 and/or Ser 1013 were mutated to Ala (Supplementary Fig. 2b), expressed them in HEK-293T cells, and immunoprecipitated them with anti-HA resin. Whereas wild-type REST efficiently immunoprecipitated endogenous β-TrCP1, the REST(E1009A), REST(S1013A) and REST (E1009A/S1013A) mutants did not (Fig. 1b and Supplementary Fig. 1b), showing that Glu 1009 and Ser 1013 are required for binding to β-TrCP. Accordingly, in comparison with wild-type REST, the half-lives of REST mutants were increased in HEK-293T cells (Fig. 1c).

Because SCF$^{β-TrCP}$ mediates the ubiquitination of several proteins in specific phases of the cell cycle[12,15,18–20], we analysed the expression of REST during the cell cycle. When HeLa cells were released from a G1/S block, REST protein levels decreased in G2, at a time when the levels of cyclin A and Emi1, which are both degraded in early mitosis, were still elevated (Fig. 1d). Similar oscillations in REST expression were observed with different synchronization methods and cell types, including HCT116, U-2OS and human diploid IMR-90 fibroblasts (Supplementary Fig. 4a, b and data not shown). The proteasome inhibitor MG132 prevented the disappearance of REST in HeLa and HCT116 cells arrested in prometaphase by a spindle poison (Supplementary Fig. 5a), showing that REST degradation is mediated by the proteasome and that this degradation persists during spindle checkpoint activation. Accordingly, in contrast with wild-type REST, REST(E1009A/S1013A) is stable in prometaphase cells (Supplementary Fig. 6a, b).

MG132-treated prometaphase cells accumulated phosphorylated REST (Supplementary Fig. 5b). Moreover, REST, but not REST (E1009A/S1013A), immunopurified from prometaphase cells was ubiquitinated *in vitro* in the presence of β-TrCP (but not FBXW8) (Fig. 1e and Supplementary Fig. 5c). Finally, incubation with

λ-phosphatase completely inhibited the ubiquitination of wild-type REST (Fig. 1e). These findings indicate that REST phosphorylation is necessary for its ubiquitination.

To further test whether β-TrCP regulates the stability of REST, we used a double-stranded RNA (dsRNA) oligonucleotide that efficiently targets both β-TrCP1 and β-TrCP2 (refs 14, 15, 18) to decrease their expression in HeLa cells. β-TrCP knockdown inhibited the G2-specific degradation of REST (Fig. 1f). Moreover, phosphorylated REST accumulated after β-TrCP silencing (Supplementary Fig. 5b).

Together, the above results demonstrate that β-TrCP-mediated degradation of REST starts in G2, and this event requires the DEGXXS degron in the REST C terminus.

Because REST is a transcriptional repressor, we proposed that its degradation in G2 might be necessary to derepress genes involved in mitosis. We therefore analysed the expression of proteins regulating mitosis and/or cell proliferation in U-2OS cells expressing either wild-type REST or REST(E1009A/S1013A). Prometaphase U-2OS cells showed higher levels of REST(E1009A/S1013A) than wild-type REST (Fig. 2a) as a result of its stabilization (Supplementary Fig. 6a, b).
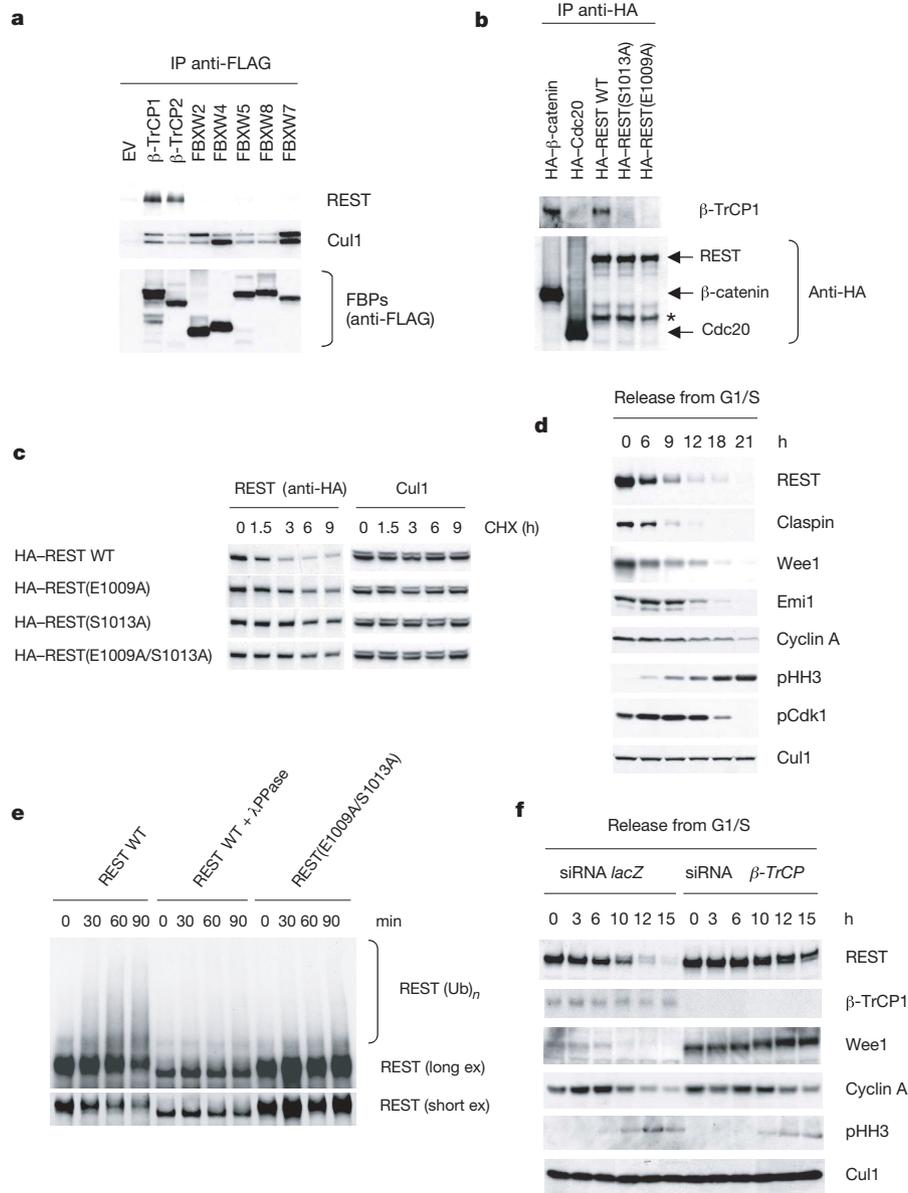


Figure 1 | REST is targeted for degradation by SCF^β-TrCP during G2. a, HEK-293T cells were transfected with empty vector (EV) or the indicated FLAG-tagged F-box protein constructs (FBPs). Cell extracts were immunoprecipitated (IP) with anti-FLAG resin, and immunocomplexes were probed for the indicated proteins. b, The indicated HA-tagged proteins were expressed in HEK-293T cells. Cell extracts were subjected to immunoprecipitation with anti-HA resin followed by immunoblotting. The asterisk indicates a non-specific band. WT, wild type. c, The indicated HA-tagged proteins were expressed in HEK-293T. At 24 h after transfection, cells were treated with cycloheximide (CHX). Cells were collected and proteins were analysed by immunoblotting with an anti-HA antibody (left panels) to detect REST or with an anti-Cul1 antibody (right panels) to show loading normalization. d, HeLa cells were synchronized by a double-thymidine block and released into nocodazole-containing medium. Cells were collected at the

indicated times, lysed and immunoblotted. e, β-TrCP-mediated REST ubiquitination is dependent on phosphorylation. HeLa cells were infected with lentiviruses expressing HA-tagged wild-type REST or HA-tagged REST(E1009/S1013A), synchronized in prometaphase and incubated with MG132 during the last 3 h before lysis. Cell extracts were immunoprecipitated with anti-HA resin. Immunoprecipitates were incubated with either λ-protein phosphatase (λPPase) or enzyme buffer before ubiquitination/degradation assays (at 30 °C for the indicated times) in the presence of in vitro transcribed/translated β-TrCP. The bracket marks a ladder of bands corresponding to polyubiquitinated REST detected by immunoblotting. ex, exposure. f, HeLa cells were transfected twice with short interfering RNA (siRNA) molecules to a non-relevant mRNA (lacZ) or to β-TrCP mRNA and then synchronized and analysed as in d.

Of the 37 proteins analysed, only the levels of Mad2 were altered in cells expressing REST(E1009A/S1013A) (Fig. 2a, and data not shown). Lower levels of Mad2 were also observed when the stable REST mutant was expressed in IMR-90 fibroblasts (Supplementary Fig. 7) and NIH 3T3 cells (data not shown). Mad2 is a crucial component of the spindle checkpoint, inhibiting the anaphase-promoting complex to prevent sister-chromatid separation until

microtubules radiating from the spindle poles have been attached to all kinetochores[21]. Northern blot analysis showed downregulation of *Mad2* mRNA in REST(E1009A/S1013A)-expressing cells (Fig. 2b). Analysis of the *Mad2* genomic sequence showed several putative RE1 sites. Chromatin immunoprecipitation analysis confirmed *in vivo* binding of endogenous REST to the *Mad2* promoter (Fig. 2c). In addition, a human *Mad2* genomic fragment containing an RE1 site (position 26–46 relative to the transcription start site), but not one containing a deletion in the RE1 site, conferred REST responsiveness to a luciferase reporter after the transient transfection of U-2OS or IMR-90 cells (Fig. 2d and Supplementary Fig. 8). Dominant-negative
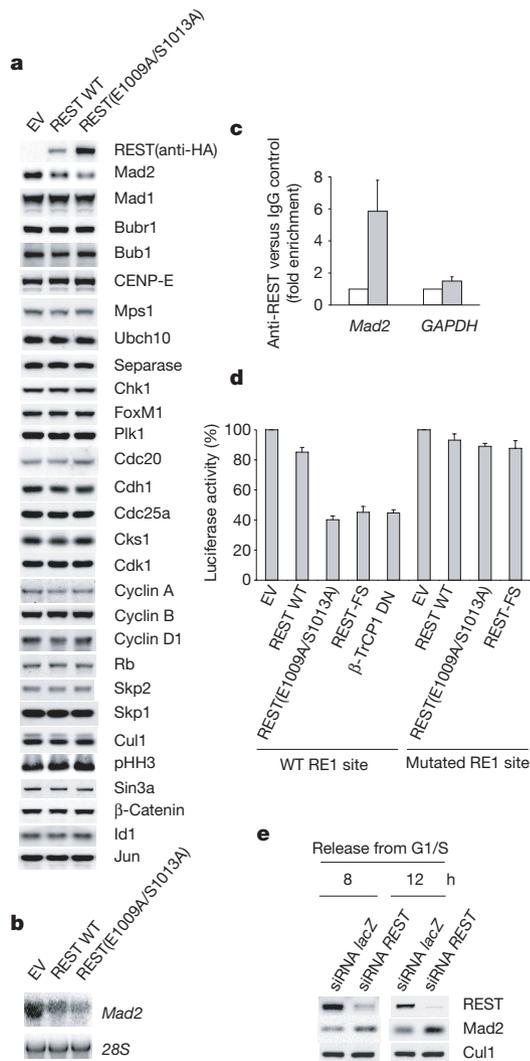


**Figure 2 | *Mad2* is a transcriptional target of REST. a**, U-2OS cells were infected either with an empty lentivirus (EV) or with lentiviruses expressing HA-tagged wild-type REST or HA-tagged REST(E1009/S1013A). After treatment with nocodazole for 15 h, mitotic cells were harvested and analysed by immunoblotting for the indicated proteins. **b**, *Mad2* mRNA was assessed by northern blotting in U-2OS cells treated as in **a**. **c**, Chromatin immunoprecipitation (ChIP) assay with an anti-REST antibody (filled columns) in U-2OS cells. Quantitative real-time PCR amplifications were performed with primers surrounding the RE1 site in the *Mad2* promoter. The value given for the amount of PCR product present from ChIP with control IgG (open columns) was set as 1. GAPDH primers were used as a negative control. **d**, U-2OS cells were transfected with an empty vector (EV), HA-tagged REST proteins or a dominant-negative β-TrCP1 mutant (FLAG–β-TrCP1 DN) together with a luciferase reporter linked to a *Mad2* genomic fragment containing either a wild-type (WT) or a mutated RE1 site. Prometaphase cells were collected and the relative luciferase signal was quantified. The value given for luciferase activity in EV-transfected cells was set at 100%. **e**, IMR-90 cells were transfected twice with siRNA molecules to a non-relevant mRNA (*lacZ*) or to *REST* mRNA and synchronized in G2 by release from an aphidicolin block for the indicated durations[30]. Cells were then lysed and immunoblotted. Where present, error bars represent s.d. (*n* = 3).

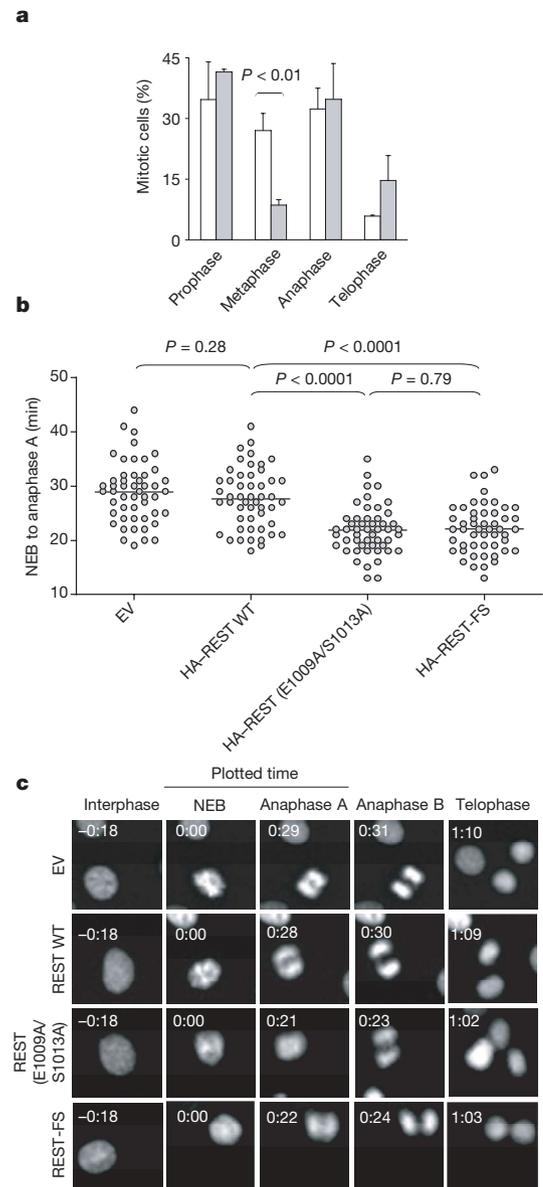**Figure 3 | Failure to degrade REST causes defects in the mitotic checkpoint. a**, HCT116 cells were infected either with an empty lentivirus (EV, open columns) or with a lentivirus expressing REST(E1009A/S1013A) (filled columns). At 48 h after infection, cells were fixed and stained with 4,6-diamidino-2-phenylindole and an anti-α-tubulin antibody to reveal DNA and the mitotic spindle, respectively. Error bars represent s.d. (*n* = 3). **b**, NIH 3T3 cells stably transfected with enhanced green fluorescent protein-labelled histone H2B were infected with an empty lentivirus or with lentiviruses expressing the indicated HA-tagged proteins. The average time from nuclear envelope breakdown (NEB) to anaphase onset was measured by time-lapse microscopy. Each symbol in the scatter plot represents a single cell. **c**, Representative fluorescence videomicroscopy series from **b**; numbers in the top left are times (h:min).

367

β-TrCP[22], which stabilizes endogenous REST (data not shown), inhibited the activity of the *Mad2* promoter-driven luciferase reporter (Fig. 2d). Importantly, depletion of REST in G2 IMR-90 cells induced an increase in Mad2 levels (Fig. 2e).

These results indicate that *Mad2* is a direct and physiologically relevant transcriptional target of REST. Consistent with this notion, *Mad2* expression (both at the mRNA and protein level) is inversely proportional to REST protein levels during the progression of cells through G2 (Supplementary Fig. 4b, c).

Deletion of a single *Mad2* allele in mouse embryonic fibroblasts or human HCT116 cancer cells results in a defective mitotic checkpoint[23]. To study whether failure to degrade REST in G2 also affects the spindle checkpoint, we analysed HCT116 cells (which have a relatively stable karyotype) expressing HA-tagged wild-type REST or HA-tagged REST(E1009A/S1013A). As expected, wild-type REST was degraded in G2, whereas REST(E1009A/S1013A) was stable in G2 (Supplementary Fig. 9). Cells expressing REST (E1009A/S1013A) showed a decreased percentage of metaphases (Fig. 3a). Because this effect might have been due to a faster progression through metaphase, we analysed mitotic progression by time-lapse microscopy. The average time from nuclear envelope breakdown to anaphase onset was decreased in cells expressing REST(E1009A/S1013A) in comparison with control cells (Fig. 3b, c and Supplementary Fig. 10). Moreover, expression of the stable REST mutant increased the number of lagging chromosomes and chromosome bridges in anaphase (Fig. 4a) and the appearance of tetraploidy (11/61 versus 0/61 in control cells), as scored in metaphase spreads from two different experiments. More than 8% of cells expressing the stable REST mutant (6/71) displayed prematurely separated sister chromatids, in contrast with 1.4% (1/71) in control cells (Fig. 4b). Finally, cells expressing the stable REST mutant showed a decrease in the mitotic index in the presence of a spindle poison, despite the fact that they entered into mitosis with normal kinetics (Fig. 4c and Supplementary Fig. 11), suggesting an increased rate of mitotic slippage and adaptation to the spindle checkpoint.

These phenotypes indicate that in cells expressing the stable REST mutant, anaphase proceeds faster and in the absence of complete and accurate chromosome–microtubule attachment. Premature anaphase and chromosome aberrations are hallmarks of the defective spindle checkpoint observed in *Mad2*^{+/−} cells[23].

We predicted that REST-FS, an oncogenic frame-shift mutant from a colon cancer cell line[11], would be stabilized because it lacks the β-TrCP degron. Indeed, we found that REST-FS did not bind β-TrCP and was stable in G2 HCT116 cells (Supplementary Figs 1b and 12a). Expression of REST-FS in U-2OS cells caused a decrease in *Mad2* mRNA and Mad2 protein (Supplementary Fig. 12b, c) and a decrease in the activity of a *Mad2* promoter-driven luciferase reporter (Fig. 2d), similarly to the expression of REST(E1009A/S1013A). Finally, the mitotic phenotypes induced by the expression of REST-FS (Figs 3b, c and 4) were indistinguishable from those caused by REST(E1009A/S1013A).

We show here that β-TrCP-mediated degradation of REST in G2 is necessary for the optimal expression of *Mad2*. Failure to degrade REST produces a deficient spindle checkpoint and consequent chromosome instability. REST is expressed in non-neuronal cells and stem/progenitor neural cells, in which it inhibits neuronal differentiation by blocking the expression of neuron-specific genes[2,24]. The transition from embryonic stem cell to stem/progenitor neuronal cell requires the proteasome-mediated degradation of REST[24]. Our study suggests that REST proteolysis must be accurately controlled to avoid subjecting neuronal tissues to cancer risk. In fact, increased levels of REST resulting from overproduction and/or C-terminal truncations, as observed in human neuronal tumours[3–7,10], would both inhibit differentiation and generate chromosomal instability, two mechanisms that contribute to tumour development. Although REST has oncogenic properties in neuronal cells, the reduction of REST expression in certain non-neuronal tumours suggests a tumour suppressor role for REST and a function in the neuroendocrine phenotype in some of these lesions[11,25]. C-terminally truncated REST variants are also observed in non-neuronal tumours[8–11]. Our study suggests that these stable REST variants may contribute to cell
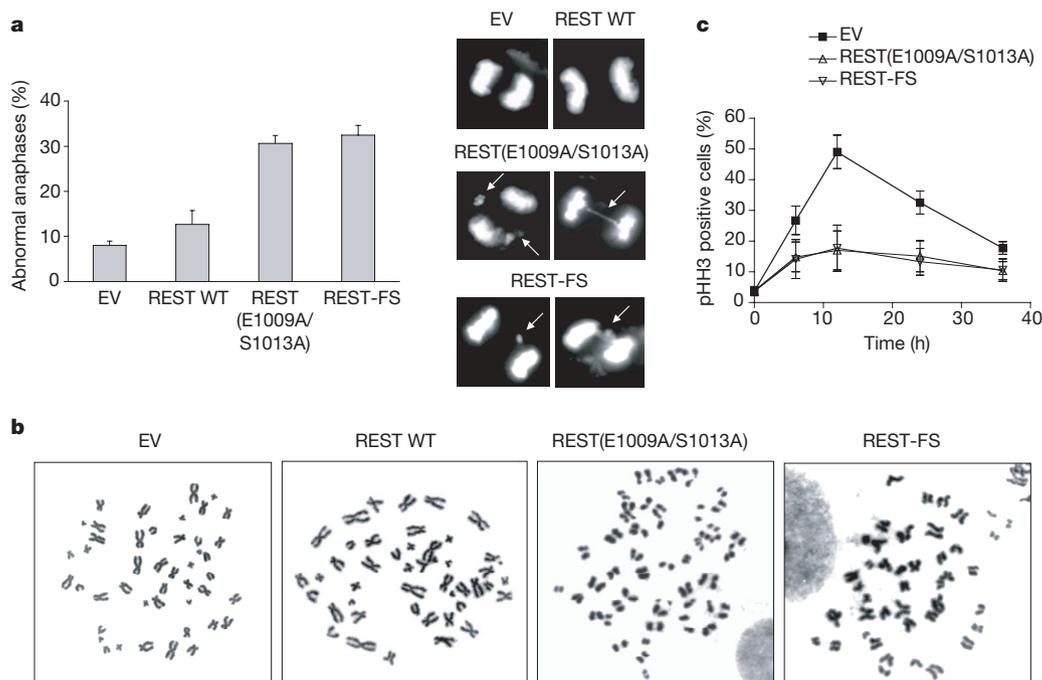


**Figure 4** | **Expression of a stable REST mutant or oncogenic REST-FS leads to chromosomal instability. a**, Left: percentage of aberrant anaphases in HCT116 cells infected as in Fig. 3b. Right: representative pictures. Arrows point to lagging chromosomes and chromosome bridges. **b**, Premature sister-chromatid separation in cells expressing stable REST. Panels show representative metaphase spreads in HCT116 cells infected as in Fig. 3b. **c**, Nocodazole was added for the indicated durations to HCT116 cells infected as in Fig. 3b. Cells were stained with an anti-phospho-HH3 (pHH3) antibody to quantify their mitotic index. Where present, error bars represent s.d. ($n = 3$).

transformation by promoting aneuploidy[26] and genetic instability in both neuronal and non-neuronal tissues.

## METHODS SUMMARY

**Biochemical methods.** Extract preparation, immunoprecipitation and immunoblotting were as described previously[14,15,18].

**Transient transfections and lentivirus-mediated gene transfer.** HEK-293T cells were transfected by using calcium phosphate. U-2OS cells were transfected with the use of FuGENE-6 reagent (Roche). For lentivirus-mediated gene transfer, HEK-293T cells were co-transfected with pTRIP-PGK together with packaging vectors. At 48 h after transfection, virus-containing medium was collected and supplemented with $8\,\mu g\,ml^{-1}$ Polybrene (Sigma). Cells were then infected with the viral supernatant for 6 h.

**Transcription analyses.** RNA was extracted by using the RNeasy Kit (Qiagen). cDNA synthesis was performed with Superscript III (Invitrogen). Quantitative real-time PCR analysis was performed in accordance with standard procedures, using SYBR Green mix (Bio-Rad). Mad2 primer sequences were reported previously[27]. Control ARPP P0 primers sequences were 5′-GCACTGGAAGTC-CAACTACTTC-3′ and 5′-TGAGGTCCTCCTTGGTGAACAC-3′. Northern blotting was performed as described[28]. $^{32}$P-labelled human full-length *Mad2* complementary DNA was used as a probe to detect *Mad2* mRNA. For luciferase assays, U-2OS cells were transfected in a 4:2:1 ratio with HA-tagged REST constructs, luciferase reporter plasmid (pGL3-Mad2)[27] and pCMV-β-galactosidase. Luciferase activity was measured with the Luciferase Reporter Assay System (Promega), and relative luciferase activities were normalized to *lacZ*.

**Chromatin immunoprecipitations.** Chromatin immunoprecipitations were conducted as described previously[29]. Mad2 primer sequences were as reported previously[27]. Glyceraldehyde-3-phosphate dehydrogenase (GAPDH) primer sequences were 5′-TCCACCACCCTGTTGCTGTA-3′ and 5′-ACCACAGTCC-ATGCCATCAC-3′.

**Full Methods** and any associated references are available in the online version of the paper at www.nature.com/nature.

Received 1 November 2007; accepted 9 January 2008.

1.  Ballas, N. & Mandel, G. The many faces of REST oversee epigenetic programming of neuronal genes. *Curr. Opin. Neurobiol.* **15**, 500–506 (2005).
2.  Ooi, L. & Wood, I. C. Chromatin crosstalk in development and disease: lessons from REST. *Nature Rev. Genet.* **8**, 544–554 (2007).
3.  Su, X. *et al.* Abnormal expression of REST/NRSF and Myc in neural stem/progenitor cells causes cerebellar tumors by blocking neuronal differentiation. *Mol. Cell. Biol.* **26**, 1666–1678 (2006).
4.  Fuller, G. N. *et al.* Many human medulloblastoma tumors overexpress repressor element-1 silencing transcription (REST)/neuron-restrictive silencer factor, which can be functionally countered by REST-VP16. *Mol. Cancer Ther.* **4**, 343–349 (2005).
5.  Higashino, K., Narita, T., Taga, T., Ohta, S. & Takeuchi, Y. Malignant rhabdoid tumor shows a unique neural differentiation as distinct from neuroblastoma. *Cancer Sci.* **94**, 37–42 (2003).
6.  Lawinger, P. *et al.* The neuronal repressor REST/NRSF is an essential regulator in medulloblastoma cells. *Nature Med.* **6**, 826–831 (2000).
7.  Nishimura, E., Sasaki, K., Maruyama, K., Tsukada, T. & Yamaguchi, K. Decrease in neuron-restrictive silencer factor (NRSF) mRNA levels during differentiation of cultured neuroblastoma cells. *Neurosci. Lett.* **211**, 101–104 (1996).
8.  Gurrola-Diaz, C., Lacroix, J., Dihlmann, S., Becker, C. M. & von Knebel Doeberitz, M. Reduced expression of the neuron restrictive silencer factor permits transcription of glycine receptor α1 subunit in small-cell lung cancer cells. *Oncogene* **22**, 5636–5645 (2003).
9.  Neumann, S. B. *et al.* Relaxation of glycine receptor and onconeural gene transcription control in NRSF deficient small cell lung cancer cell lines. *Brain Res. Mol. Brain Res.* **120**, 173–181 (2004).
10. Coulson, J. M., Edgson, J. L., Woll, P. J. & Quinn, J. P. A splice variant of the neuron-restrictive silencer factor repressor is expressed in small cell lung cancer: a potential role in derepression of neuroendocrine genes and a useful clinical marker. *Cancer Res.* **60**, 1840–1844 (2000).
11. Westbrook, T. F. *et al.* A genetic screen for candidate tumor suppressors identifies REST. *Cell* **121**, 837–848 (2005).
12. Guardavaccaro, D. & Pagano, M. Stabilizers and destabilizers controlling cell cycle oscillators. *Mol. Cell* **22**, 1–4 (2006).
13. Jin, J. *et al.* Systematic analysis and nomenclature of mammalian F-box proteins. *Genes Dev.* **18**, 2573–2580 (2004).
14. Dorrello, N. V. *et al.* S6K1- and βTRCP-mediated degradation of PDCD4 promotes protein translation and cell growth. *Science* **314**, 467–471 (2006).
15. Peschiaroli, A. *et al.* SCF$^{\beta TrCP}$-mediated degradation of Claspin regulates recovery from the DNA replication checkpoint response. *Mol. Cell* **23**, 319–329 (2006).
16. Cardozo, T. & Pagano, M. The SCF ubiquitin ligase: insights into a molecular machine. *Nature Rev. Mol. Cell Biol.* **5**, 739–751 (2004).
17. Wu, G. *et al.* Structure of a β-TrCP1–Skp1–β-catenin complex: destruction motif binding and lysine specificity of the SCF$^{\beta-TrCP1}$ ubiquitin ligase. *Mol. Cell* **11**, 1445–1456 (2003).
18. Guardavaccaro, D. *et al.* Control of meiotic and mitotic progression by the F box protein β-Trcp1 *in vivo*. *Dev. Cell* **4**, 799–812 (2003).
19. Busino, L. *et al.* Degradation of Cdc25A by β-TrCP during S phase and in response to DNA damage. *Nature* **426**, 87–91 (2003).
20. Watanabe, N. *et al.* Ubiquitination of somatic Wee1 by SCFβTrcp is required for mitosis. *Proc. Natl Acad. Sci. USA* **101**, 4419–4424 (2004).
21. Nasmyth, K. How do so few control so many? *Cell* **120**, 739–746 (2005).
22. Latres, E., Chiaur, J. & Pagano, M. The human F box protein β-Trcp associates with the Cul1/Skp1 complex and regulates the stability of β-catenin. *Oncogene* **18**, 849–854 (1999).
23. Michel, L. S. *et al.* MAD2 haplo-insufficiency causes premature anaphase and chromosome instability in mammalian cells. *Nature* **409**, 355–359 (2001).
24. Ballas, N., Grunseich, C., Lu, D. D., Speh, J. C. & Mandel, G. REST and its corepressors mediate plasticity of neuronal gene chromatin throughout neurogenesis. *Cell* **121**, 645–657 (2005).
25. Majumder, S. REST in good times and bad: roles in tumor suppressor and oncogenic activities. *Cell Cycle* **5**, 1929–1935 (2006).
26. Pellman, D. Aneuploidy and cancer. *Nature* **446**, 38–39 (2007).
27. Hernando, E. *et al.* Rb inactivation promotes genomic instability by uncoupling cell cycle progression from mitotic control. *Nature* **430**, 797–802 (2004).
28. Kudo, Y. *et al.* Role of F-box protein βTrcp1 in mammary gland development and tumorigenesis. *Mol. Cell. Biol.* **24**, 8184–8194 (2004).
29. Busino, L. *et al.* SCFFbxl3 controls the oscillation of the circadian clock by directing the degradation of cryptochrome proteins. *Science* **316**, 900–904 (2007).
30. Amador, V., Ge, S., Santamaria, P., Guardavaccaro, D. & Pagano, M. APC/C$^{Cdc20}$ controls the ubiquitin-mediated degradation of p21 in prometaphase. *Mol. Cell* **27**, 462–473 (2000).

369

## METHODS

**Cell culture, synchronization and drug treatments.** U-2OS, HCT116, HEK-293T, HeLa and IMR-90 cells were grown, synchronized and treated with drugs as described previously[14,15,18].

**Purification of β-TrCP interactors.** An immunoaffinity/enzymatic assay that enriches for ubiquitinated substrates of F-box proteins, followed by mass spectrometry analysis, was described previously[14,15].

**Antibodies.** Anti-Mad2 and anti-REST antibodies were provided by H. Yu and by G. Mandel, respectively. Commercially available antibodies were as follows: anti-REST-C (Upstate 07-579), anti-Mad2 (BD 610679), anti-Cul1 (Zymed 32-2400), anti-phospho-histone H3 (anti-pHH3; Upstate 06-570), anti-M2 FLAG (Sigma F3165), anti-Cdk1 phosphorylated on Tyr 15 (pCdk1; Santa Cruz sc-7989-R), anti-phospho MPM2 (Upstate 05-368), and anti-α-Tubulin (Zymed 32-2500). All additional antibodies used here were described previously[14,15,18].

**Vectors.** Human REST cDNA was provided by G. Mandel and N. Ballas and subcloned into pcDNA3.1. REST mutants were generated using the QuickChange Site-directed Mutagenesis kit (Stratagene). Enhanced green fluorescent protein-labelled histone H2B cloned into pEGFP-N1 was provided by I. Sanchez. For lentivirus production, both wild-type REST and REST mutants were subcloned into the lentivirus vector pTRIP, which was provided by D. Levy.

**Gene silencing by small interfering RNA.** siRNA for *β-TrCP* was described previously[14,15,18]. A 21-nucleotide siRNA duplex corresponding to a non-relevant gene (*lacZ*) was used as control.

**Indirect immunofluorescence.** Cells were plated and cultured on chambered glass tissue-culture slides (BD Falcon) with complete medium. Cells were washed in PBS, fixed and permeabilized in 100% methanol at −20 °C for 10 min and then incubated with the primary antibodies for 1 h at 25 °C in 0.5% Tween 20 in PBS (0.5% TBST). Slides were washed three times in 0.5% TBST for 5 min and incubated with secondary antibodies diluted 1:1,000. 4,6-Diamidino-2-phenylindole (Molecular Probes) was included to reveal nuclei. Slides were washed in PBS and subsequently mounted with Aqua Poly/Mount (Polysciences). Images were acquired with a Nikon Eclipse E800 fluorescence deconvolution microscope.

**Live cell imaging.** Live cell imaging was performed as described previously[27].

**Chromosome analysis.** Chromosome analysis of cells in metaphase was performed as described[23].

*In vitro* **ubiquitination/degradation assay.** HA-tagged wild-type REST or HA-tagged REST(E1009/S1013A) were immunoprecipitated with anti-HA antibody from HeLa cells infected with lentiviruses expressing HA-tagged wild-type REST or HA-tagged REST(E1009/S1013A), treated with nocodazole for 15 h and with MG132 for the last 3 h. Immunoprecipitates were incubated with either λ phosphatase or phosphatase buffer for 1 h at 30 °C. *In vitro* ubiquitination/degradation assays were performed by adding to agarose beads 10 μl containing 50 mM Tris-HCl pH 7.6, 5 mM MgCl$_2$, 0.6 mM dithiothreitol, 2 mM ATP, 1.5 ng μl$^{-1}$ E1 (Boston Biochem), 10 ng μl$^{-1}$ Ubc3, 10 ng μl$^{-1}$ Ubc5, 2.5 μg μl$^{-1}$ ubiquitin (Sigma), 1 μM ubiquitin aldehyde and 2 μl of unlabelled *in vitro* transcribed/translated β-TrCP1 or FBXW8. The reactions were then incubated at 30 °C for the indicated durations and analysed by immunoblotting with an anti-HA antibody.

**Interaction models.** All-atom models of all peptides were derived from the PDB structure of β-TrCP bound to β-catenin (PDB: 1p22) using a stochastic global optimization in internal coordinates with pseudo-brownian and collective probability-biased random moves as implemented in the ICM 3.0 program (Molsoft; ICM software manual, Version 3.0, 2004). The energy function used to calculate the interaction energy of phosphoserine and mutations with β-TrCP uses ECEPP/3 force-field parameters[31]:

$$E = E_{el} + E_{hb}$$

in which $E_{hb}$ is an original ECEPP/3 energy function. The electrostatics term $E_{el}$ was calculated by using the boundary element method with ECEPP/3 atomic charges and an internal dielectric constant of 4.0 (ref. 32). The same energy function was used to assess 54 crystallographically resolved phosphoserines containing only one contacting arginine and bound at protein interaction sites from the Protein Data Bank. The mean and one standard deviation of the range of energy values is shown by the vertical green line in Supplementary Fig. 3.

31. Nemethy, G. *et al.* Energy parameters in polypeptides. 10. Improved geometric parameters and nonbonded interactions for use in the ECEPP/3 algorithm with application to proline-containing peptides. *J. Phys. Chem.* **96**, 6472–6484 (1992).
32. Totrov, M. & Abagyan, R. Rapid boundary element solvation electrostatics calculations in folding simulations: successful folding of a 23-residue peptide. *Biopolymers* **60**, 124–133 (2001).